Mustafa Zor[1,5], Ferhat Şen[2], Erdal Eroğlu[3], Zeki Candan[4,5]

Triboelectric and Hydrophobic Characterization of Functionalized Lignocellulosic Materials

Triboelektrična i hidrofobna svojstva funkcionaliziranih lignoceluloznih materijala

ORIGINAL SCIENTIFIC PAPER
Izvorni znanstveni rad
Received – prispjelo: 12. 1. 2023.
Accepted – prihvaćeno: 6. 6. 2023.
UDK: 630*81
https://doi.org/10.5552/drvind.2023.0084

ABSTRACT • *In the development of sustainable products, lignocellulosic materials with hydrophobic properties can be functionalized and used as reinforcement, especially in bio-composite materials, as well as in various applications such as packaging, water-repellent and self-renewing materials. This study is aimed to improve the surface properties and triboelectric properties of wood materials. Functionalized wood veneers were prepared by impregnating 3 different wood veneers (beech, mahogany and oak) with 5 different chemical solutions (cationic cellulose, cationic starch, polyethyleneimine, sodium alginate and carboxymethyl cellulose). Structural characterization of the functional wood materials obtained was investigated by Fourier-transform infrared spectroscopy (FT-IR) technique, wettability and surface properties were examined by contact angle measurements, and morphological properties were examined by scanning electron microscopy (SEM). The triboelectric properties of the devices prepared using functionalized wood materials were investigated. As a result, it was determined that the hydrophobic properties of wood materials were improved and showed triboelectric properties. It demonstrates that functionalized wood materials can be used to power low-power electronic devices.*

KEYWORDS: *lignocellulosic materials, triboelectric properties, surface properties*

SAŽETAK • *U razvoju održivih proizvoda lignocelulozni materijali hidrofobnih svojstava mogu se funkcionalizirati i upotrebljavati kao ojačivači u biokompozitnim materijalima ili mogu imati različitu primjenu u ambalaži te u vodoodbojnim i samoobnavljajućim materijalima. Cilj ovog istraživanja bio je pronaći način poboljšanja površinskih i triboelektričnih svojstava drvnih materijala. Za istraživanje je pripremljen funkcionalizirani furnir od tri različite vrste drva (bukovine, mahagonija i hrastovine), impregniran s pet različitih kemijskih otopina (kationskom celulozom, kationskim škrobom, polietileniminom, natrijevim alginatom i karboksimetilcelulozom). Karakterizacija strukture dobivenih funkcionaliziranih drvnih materijala provedena je Furierovom infracrvenom spektroskopijom (FT-IR), kvašenje i svojstva površine istražena su mjerenjem kontaktnog kuta, a morfološka svojstva ispitana su skenirajućim elektronskim mikroskopom (SEM). Nadalje, istražena su triboelektrična svojstva uređaja izrađenih od funkcionaliziranih drvnih materijala. Utvrđeno je da se funkcionalizirani drvni materijali mogu primijeniti za napajanje uređaja male snage.*

KLJUČNE RIJEČI: *lignocelulozni materijali, triboelektrična svojstva, svojstva površine*

[1] Author is researcher at Zonguldak Bulent Ecevit University, Department of Forestry, Zonguldak, Türkiye. https://orcid.org/0000-0002-2115-8339
[2] Author is researcher at Zonguldak Bulent Ecevit University, Department of Food Processing, Zonguldak, Türkiye. https://orcid.org/0000-0001-7733-2263
[3] Author is researcher at Manisa Celal Bayar University, Faculty of Engineering, Department of Bioengineering, Manisa, Türkiye. https://orcid.org/0000-0001-7281-3906
[4] Author is researcher at İstanbul University-Cerrahpaşa, Department of Forest Industrial Engineering, İstanbul, Türkiye.
[5] Authors are researchers at Biomaterials and Nanotechnology Research Group & BioNanoTeam, Istanbul, Türkiye. https://orcid.org/0000-0002-4937-7904

1 INTRODUCTION
1. UVOD

Wood is used in many applications due to its excellent mechanical properties, relative abundance and being a renewable resource. Cellulose, hemicellulose, and lignin are the main components of wood. There is a distinct color difference between carbohydrates and phenolics. Lignin, a phenolic compound, is much darker in color than cellulose and hemicellulose (Zhu *et al.,* 2016). Wooden surfaces in real use are susceptible to being affected by external factors that change their technological properties. The wood material is hydrophilic, and its hygroscopicity and dimensional stability change after the water binds to the wood surface, causing some defects in the wood material (Engelund *et al.,* 2013; Rautkari *et al.,* 2013; Keplinger *et al.,* 2015). Lignocellulosic materials with hydrophobic properties are of great interest to develop sustainable products that can be used in various applications such as packaging, water-repellent, and self-cleaning materials, oil and water separation, or as supplements in bio-composite materials. The hydroxyl functional groups present in cellulose provide the possibility to perform various chemical modifications to cellulosic substrates that can increase their hydrophobicity (Rodríguez-Fabià *et al.,* 2022).

Wood is a biodegradable material. It is environmentally friendly, renewable, abundant and inexpensive. Wood can be transformed into flexible wood-based micro or nanomaterials after being chemically processed. Its porous structure and unique properties (high mechanical properties, high surface area, high aspect ratio, and low density) pave the way for the use of wood and wood-derived materials in triboelectric nanogenerators (TENGs) (Chen *et al.,* 2018. TENGs display many advantageous features such as being light and miniaturized, not adversely affecting aesthetic and comfort properties, and having a wide range of materials. In recent years, many studies have been carried out on TENGs due to their low weight, small size, flexibility, many material options, useful design structures and superior performance at low frequencies (Chen *et al.,* 2018; Wang, 2022); Sun *et al.,* (2021) fabricated and characterized TENG devices using triboelectrically negative polydimethylsiloxane and triboelectrically positive zeolitic imidazolate framework-8. They reported that the devices they designed could be used to power smart buildings, household lamps, calculators, and electronic windows. In another study, Wang *et al.,* (2022) fabricated TENGs from lignin-based nanofibers produced using the electro-spinning technique. They emphasized that the effect of these lignin-based high performance tribopositive materials is important in sustainable energy.

The aim of this study is to improve the triboelectric behavior and hydrophobic properties of wood coatings. Functional wood veneers were obtained by impregnating 3 wood veneer types (beech, mahogany and oak) with 5 different chemicals (cationic cellulose, cationic starch, polyethyleneimine, sodium alginate and carboxymethyl cellulose). The surface properties and triboelectric properties of the obtained functional wood veneers were investigated, and their chemical structure, surface properties and morphology were also characterized.

2 MATERIALS AND METHODS
2. MATERIJALI I METODE

2.1 Material
2.1. Materijal

Oak, Beech and Mahogany wood veneers (0.75 mm thickness) were supplied from Rasmus Farschs Vej (Denmark) company. Corn starch (unmodified regular corn starch containing approximately 73 % amylopectin and 27 % amylose), hydroxyethyl cellulose (average Mv ~90000), glycidyl trimethylammonium chloride (GTAC), sodium alginate, sodium hydroxide (NaOH), isopropyl alcohol, poly(ethyleneimine) solution, carboxymethylcellulose sodium salt were purchased from Sigma Aldrich. Ethanol was purchased from Merck. All reagents were used without further purification.

2.2 Preparation of solutions
2.2. Priprema otopina

Five different coating solutions were used to impregnate the wood. First, cationic starch (CS) and cationic cellulose (CC) were synthesized and characterized according to previous methods in the literature.

5 g of corn starch, 2.5 g of GTAC, 1.5 mL of 1 mol/L NaOH solution and 1.625 g of distilled water were added to a flask. The flask was incubated in a 60 °C water bath for 5 hours. At the end of this time interval, the reaction was stopped by adding 100 mL of ethanol to the flask and CS was precipitated. The precipitated CS was filtered in vacuum and washed with ethanol. CS was dried in an oven at 50 °C for 6 hours and milled. CS was obtained as a white powder (Şen *et al.,* 2017). CC was synthesized by the same method as CS. Isopropanol was used as the solvent instead of distilled water (Şen and Kahraman, 2018).

20 % aqueous solutions of 4 CS and CC, 10 % aqueous solutions of sodium alginate (SA) and carboxymethyl cellulose (CMC), 25 % aqueous solutions of polyethyleneimine (PEI) were prepared.

2.3 Applying solutions to samples
2.3. Nanošenje otopina na uzorke

Beech (B), Mahogany (M), and Oak (O) veneers were cut in 7 cm × 3.5 cm dimensions. 20 ml of 5 different solutions prepared for each coating type was

poured on the tested wood. It was spread homogeneously with the in-situ growth technique. Wood coatings were dried in an oven at 50 °C for 24 hours. In total, 15 different samples (3 different kinds of wood coated by 5 different coating materials) were obtained. All samples were systematically coded. For example, the sample with beech veneer impregnated with cationic cellulose was coded as BCS, while the sample with sodium alginate impregnation on oak veneer was coded as OSA.

2.4 Device fabrication
2.4. Izrada uređaja

Triboelectric devices were prepared by using wooden materials impregnated with anionic and cationic solutions. All wood veneers were used in pairs with each other according to Sun *et al.* (2021) method to determine the best triboelectric performing device. 15 different wood coatings impregnated with solution were covered with 1 mm thick commercial copper foil to conduct electricity. The solution-impregnated wood veneers were joined with the copper foil-covered parts to the outside and device pairs were prepared. In this way, a total of 210 different device pairs were obtained.

2.5 Methods
2.5. Metode

Infrared (IR) spectra of coated wood materials were obtained on a Perkin Elmer UATR instrument. Each test material was directly analyzed in transmission mode in the range of 4000–400 cm^{-1} with 4 scans per sample at room temperature.

By applying a certain force to the prepared devices, the measurements of the electrical output formed in the material were taken. At the same time, a loading cell was mounted on the rigid frame of the motor to monitor the pressure applied to the samples. The electrical output was measured by a Digilent Analog Discovery 2, equipped with a WaveForms software.

The surface hydrophobicity of wood coatings was analyzed measuring the contact angle using a goniometer (Krüss Advance Drop Shape Analyzer, DSA100). The coated-wood material was cut into a thin strip before being analyzed. For the measurement of the contact angle, measurements were taken from 2 µl of distilled water (pH 7) or diiodomethane dropped on the tested wood surface. Measurements were taken within 10 seconds of instillation of drops.

The geometric mean method, which is based on the contact angle measurement of 2 different liquids deposited on a solid wood surface, was used to calculate the surface free energy of wood coatings using Eq. 1 described by Fernandez and Khayet (2015).

$$2\sqrt{\gamma_s^d \cdot \gamma_l^d} + 2\sqrt{\gamma_s^{nd} \cdot \gamma_l^{nd}} = \gamma_l(1+cosQ) \quad (1)$$

Where γ_s^d is the dispersive component of the solid; γ_l^d is the dispersive component of the liquid; γ_s^{nd} is the non-dispersive component of the solid; γ_l^{nd} is the non-dispersive component of the liquid; γ_l is the total surface free energy or surface tension of the liquid and Q is the contact angle measured between the liquid and the solid under study.

From the total surface tension and surface tension components estimated by the methods described above, the solubility parameter (δ) of wood surface coatings was calculated using the Eq.2 and Eq.3 (Fernandez and Khayet (2015)).

$$e_c = (\gamma_s / 0.75)^{3/2} \quad (2)$$

$$\delta = (e_c)^{1/2} \quad (3)$$

Where e_c (mJ/m^3) is the cohesive energy density, which is related to γ_s (mJ/m^2) as Eq. 3 (Victoria and Mohamed, 2015).

Morphology of the solution-impregnated wood coatings was determined by SEM using Phillips XL 30 ESEM-FEG microscope. Samples were cryo-fractured in liquid nitrogen, covered with a thin gold layer, and the fractured surface was examined under SEM analyses.

2.6 Statistical analyses
2.6. Statistička analiza

All measurements for the surface contact angle of water and diidomethane were repeated five times independently, and the results were expressed as means ± standard deviations. The data calculated from the surface contact angle of water and diidomethane for surface free energy and solubility parameter were analyzed using the Minitab statistical software. Statistical differences between groups were determined by the one-way ANOVA test followed by the Tukey Method (p<0.05).

3 RESULTS AND DISCUSSION
3. REZULTATI I RASPRAVA

3.1 Structural characterization of functional wood materials
3.1. Strukturna obilježja funkcionalnih drvnih materijala

The FT-IR spectra of pure beech, mahogany and oak wood coatings and chemically impregnated coatings are shown in Figure 1. When the FT-IR spectrum of the pure beech veneer is examined, bands are observed at 1736 cm^{-1} of C–O stretch in cellulose and hemicellulose and at 1032 cm^{-1} of carbonyl groups (Geffert *et al.,* 2017). In the FT-IR spectrum of undoped mahogany, the band belonging to the unconjugated carbonyl group is seen at 1743 cm^{-1} (Jian, 2003; Wang *et al.,* 2017).

Similarly, a band of unconjugated carbonyl group is seen at 1732 cm^{-1} in the FT-IR spectrum of pure oak

(Kubovský *et al.,* 2020). In the FT-IR spectra of coatings containing cationic starch, belonging to the hydroxyl group at 3275 cm^{-1}, C-H stretching vibration at 2919 cm^{-1}, C-O stretching vibration at 1148, 1076 and 996 cm^{-1}, at 1473 cm^{-1} the band of C-N stretching vibration is seen (Pal *et al.,* 2005; Şen *et al.,* 2017). Similarly, when the FT-IR spectra of wood materials containing cationic hydroxyethyl cellulose are examined, the broad band of the stretch vibrations of the hydroxyl group are observed at 3378 cm^{-1}, the band of C-H stretching vibrations at 2867 cm^{-1}, the C-O in the anhydroglucose units of hydroxyethyl cellulose at 1049 cm^{-1}. A band of stretching vibrations and a band of C-N stretching vibrations at 1475 cm^{-1} were observed (Şen and Kahraman, 2018). In the FT-IR spectra of wood materials containing sodium alginate, bands of -COO- asymmetric and symmetric stretching vibrations at 1417 cm^{-1} and 1615 cm^{-1}, and bands of -OH and C-H stretching vibrations at 2922 cm^{-1} and 3428 cm^{-1} were detected (Zhang *et al.,* 2018). In the FT-IR spectra of polyethyleneimine-containing wood coating materials, the bands of C–H bond were observed at 2836 cm^{-1} and 2947 cm^{-1}, while the band of primary amines (N-H) was observed at 1585 cm^{-1} (Linden *et al.,* 2015). In the FT-IR spectra of the samples containing carboxymethyl cellulose, the band due to the stretching frequency of the hydroxyl group was observed at 3423 cm-1, the band due to the C-H stretching vibration at 2920 cm^{-1}, the band due to the presence of COO- at 1620 cm^{-1}, 1423 and 1328 cm^{-1}. The band due to -CH_2 and hydroxyl group bending vibration around the band due to CH-O-CH_2 stretching at 1054 cm^{-1} was observed (Haleem *et al.,* 2014). The presence of specific bands of impregnated chemicals in the FT-IR spectra of wood materials proves that the chemicals are successfully impregnated on wood materials.

3.2 Triboelectric performance of devices
3.2. Triboelektrična svojstva uređaja

The images of the highest measured stresses of Beech, Mahogany, and Oak veneers are shown in Figure 2. When the obtained results were examined, it was found that PEI impregnated beech veneer and CS impregnated Mahogany veneer had the highest (1.72V) triboelectric production. It was observed that the highest values obtained were in all PEI-impregnated wood coatings. On the other hand, it is seen that devices consisting mostly of CS-impregnated wood materials and PEI-impregnated wood materials have the highest stresses. As a result, it can be interpreted that PEI and CS have the highest tribopolarity. When the relationship between wood veneer types was examined, similar results were observed in beech and mahogany, while lower strains were measured in oak. It is thought that the reason for this is that the impregnation process becomes difficult due to the formation of tulle in the anatomical structure of the oak tree. Sun *et al.* (2021) prepared tribolelectric nanogenerators by applying zeolitic imidazolate framework-8, a metal-organic framework and poly(dimethylsiloxane) to spruce veneers. They reported measuring an open circuit voltage 80 times higher than that of natural wood (spruce). This

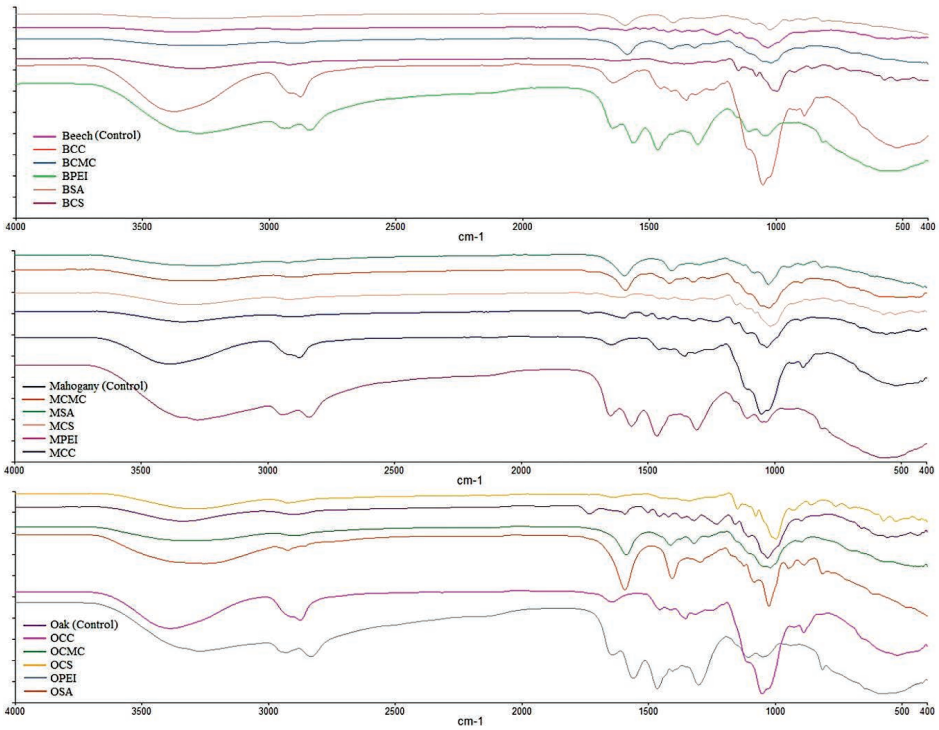

Figure 1 FT-IR spectra of all samples
Slika 1. FT-IR spektri svih uzoraka

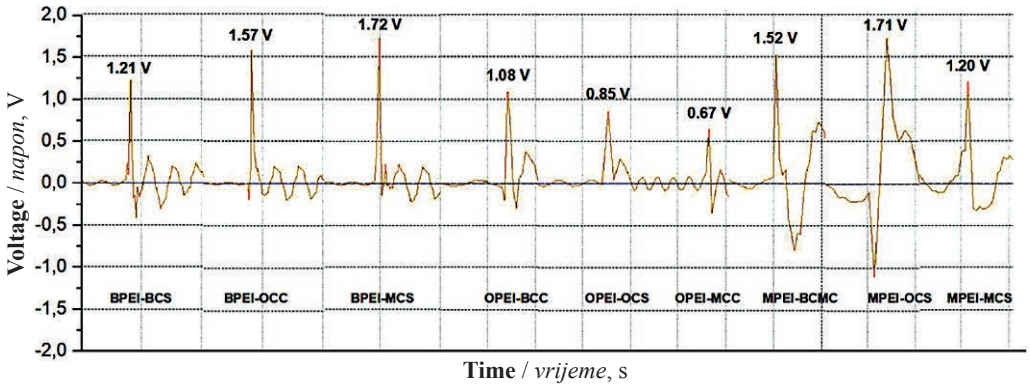

Figure 2 Triboelectric output of functionalized wood veneers
Slika 2. Triboelektrični izlaz funkcionaliziranih drvnih furnira

result is an indication that triboelectricity can be imparted to wood material by treating chemicals with various tribopolarity. It is seen that the results obtained in our study are compatible with the literature.

3.3 Contact angle and surface properties of functional wood materials

3.3. Kontaktni kut i površinska svojstva funkcionalnih drvnih materijala

Contact angle measurements were carried out to examine the wettability of pure wood veneers and the resulting functional wood veneers. The images of the contact angles of the samples with water (the closest value to the mean) are shown in Figure 3. According to the results, the highest contact angle value among all groups was measured as 105.9º in the functional material prepared by impregnating the oak veneer with cationic starch. On the other hand, the lowest contact angle value among all groups was measured as 25.7º in the functional material prepared by impregnating the beech veneer with carboxymethyl cellulose. In general, increases in contact angle values were observed with chemical impregnation of all wood coatings. Increasing the contact

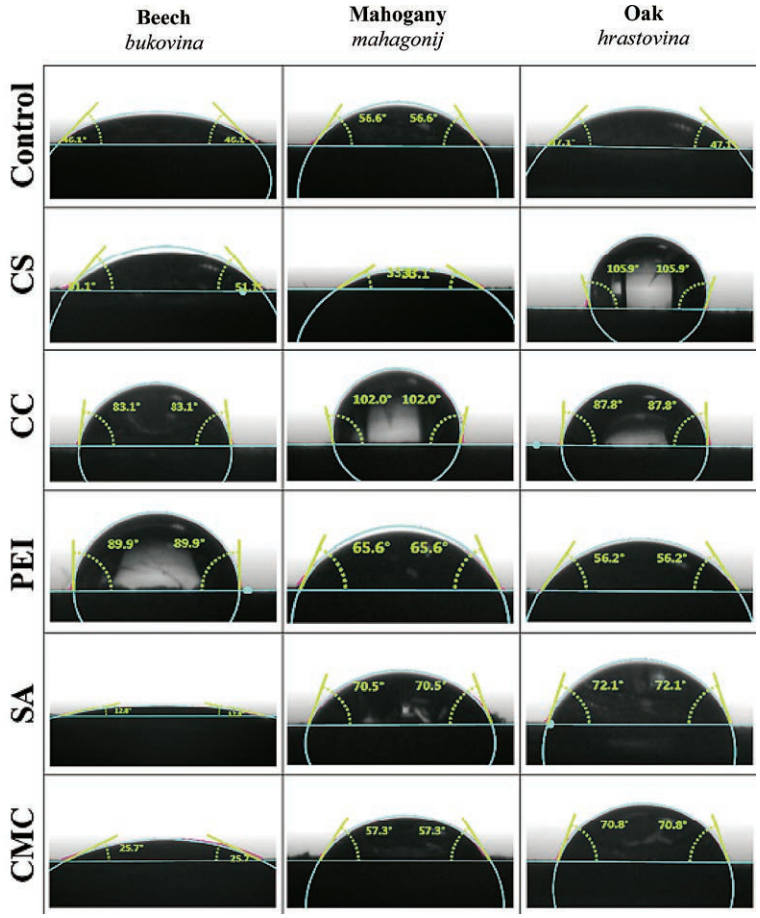

Figure 3 Contact angle images of functional wood materials with water (closest to mean)
Slika 3. Slike kontaktnog kuta vode na funkcionalnim drvnim materijalima (najbliža vrijednost srednjoj vrijednosti)

angle value gives the material a hydrophobic property and reduces its wettability (Huhtamäki *et al.,* 2018). While wooden materials are generally in contact with water, their mechanical properties decrease over time. By impregnating wood materials with chemicals, the mechanical properties of the coatings were kept stable.

Surface free energies and solubility parameters calculated from the contact angles of functional wood coatings with water and diiodomethane are shown in Table 1. The highest surface free energy in mahogany coating was observed in MCS sample as 62.25. The lowest surface free energy was calculated as 35.62 in the MPEI sample. While the highest surface free energy in beech veneer was 66.55 in BCMC sample, and the lowest surface free energy was observed in BPEI sample as 28.60. The highest surface free energy was calculated as 50.59 in the oak veneer, while the lowest surface free energy was calculated as 39.76 in the OCC sample. Similar results are valid for the calculated solubility parameter values. According to the results obtained, it is seen that the surface free energy and solubility parameter decrease with the increase of the contact angle and a more hydrophobic surface is obtained (Chieng *et al.,* 2019).

3.4 Morphology of functional wood materials
3.4. Morfologija funkcionalnih drvnih materijala

Morphological structures of pure and functionalized wood veneers were examined by scanning electron microscopy. Images of all samples at 500x magnification were used for characterization (Figure 4). When the SEM images were examined, it was determined that the chemicals impregnated on the wood coatings homogeneously filled the pores of the wood materials. Homogeneous distribution of chemicals impregnated on wood coatings is a factor that significantly affects the triboelectric and wettability properties of materials.

4 CONCLUSIONS
4. ZAKLJUČAK

In this study, triboelectric behavior and hydrophobic properties of functional wood coatings obtained by impregnating 3 different wood coatings with 5 different chemicals were examined. According to the structural characterization results, it was determined that the chemicals applied to all wood coating types were successfully impregnated. It was seen that the chemical groups showing the highest tribopolarity of the triboelectric measurements were PEI and CS, and at the same time, more tension was obtained in beech and mahogany veneer compared to oak veneer. This was measured by the BPEI-MCS device with the highest voltage of 1.72 V. The contact angle measurement results showed that the application of chemicals to wood coatings increases the wettability of the materials, that is, the hydrophobicity. The contact angle values of pure wood veneers increased from around 50 degrees to over 100 degrees af-

Table 1 Surface free energies and solubility parameters of functional wood coatings
Tablica 1. Slobodne površinske energije i parametri topljivosti funkcionalnih premaza za drvo

Sample / *Uzorak*		**Water** *Voda*	**Diiodomethane** *Dijodometan*	**Surface free energy ɤ, mJ/m²** *Slobodna površinska energija* ɤ, mJ/m²	**Solubility parameter δ, mJ$^{1/2}$/m$^{3/2}$** *Parametar topljivosti* δ, mJ$^{1/2}$/m$^{3/2}$
M	Control	$57.62^{\pm4.15}$	$43.46^{\pm2.05}$	$47.88^{\pm2.78b}$	$22.58^{\pm0.98b}$
	CC	$98.68^{\pm6.06}$	$40.92^{\pm2.51}$	$40.40^{\pm0.40c}$	$19.88^{\pm0.15c}$
	CMC	$57.10^{\pm2.52}$	$46.14^{\pm5.02}$	$47.43^{\pm2.71b}$	$22.42^{\pm0.96b}$
	CS	$33.32^{\pm5.72}$	$43.82^{\pm2.18}$	$62.10^{\pm3.02a}$	$27.44^{\pm1.00a}$
	PEI	$79.70^{\pm21.50}$	$51.02^{\pm2.05}$	$39.77^{\pm4.92c}$	$19.62^{\pm1.83c}$
	SA	$66.34^{\pm6.20}$	$41.96^{\pm6.39}$	$40.01^{\pm1.92c}$	$19.73^{\pm0.71c}$
B	Control	$44.98^{\pm2.73}$	$50.82^{\pm2.48}$	$54.13^{\pm2.12b}$	$24.76^{\pm0.73b}$
	CC	$82.00^{\pm6.70}$	$41.90^{\pm2.18}$	$39.57^{\pm2.03c}$	$19.57^{\pm0.75c}$
	CMC	$25.62^{\pm2.19}$	$40.98^{\pm2.59}$	$66.52^{\pm1.20a}$	$28.90^{\pm0.39a}$
	CS	$51.62^{\pm4.60}$	$40.30^{\pm3.45}$	$52.03^{\pm3.21b}$	$24.03^{\pm1.12b}$
	PEI	$92.36^{\pm3.27}$	$60.48^{\pm3.70}$	$28.64^{\pm2.22d}$	$15.35^{\pm0.89d}$
	SA	$14.16^{\pm3.04}$	$38.36^{\pm0.85}$	$71.04^{\pm0.85a}$	$30.36^{\pm0.27a}$
O	Control	$48.30^{\pm1.02}$	$62.90^{\pm3.13}$	$51.59^{\pm1.01a}$	$23.89^{\pm0.35a}$
	CC	$89.44^{\pm5.07}$	$39.72^{\pm1.21}$	$39.99^{\pm0.50b}$	$19.73^{\pm0.18b}$
	CMC	$71.24^{\pm3.03}$	$38.28^{\pm1.01}$	$43.39^{\pm1.30b}$	$20.98^{\pm0.47b}$
	CS	$107.20^{\pm8.64}$	$39.64^{\pm2.25}$	$43.97^{\pm1.77b}$	$21.18^{\pm0.64b}$
	PEI	$55.98^{\pm2.44}$	$42.46^{\pm4.84}$	$49.01^{\pm2.32a}$	$22.98^{\pm0.82a}$
	SA	$66.72^{\pm6.82}$	$46.62^{\pm2.71}$	$42.42^{\pm4.11b}$	$20.61^{\pm1.49b}$

All values are expressed as arithmetic mean of five different measurements, with ± standard deviation values. / *Sve su vrijednosti izražene kao aritmetička sredina pet različitih mjerenja s vrijednostima ± standardne devijacije.*
[a–d]Similar letters show no statistical difference within each group at $p<0.05$. / [a–d]*Ista slova ne pokazuju statističku razliku unutar svake skupine pri $p<0,05$.*

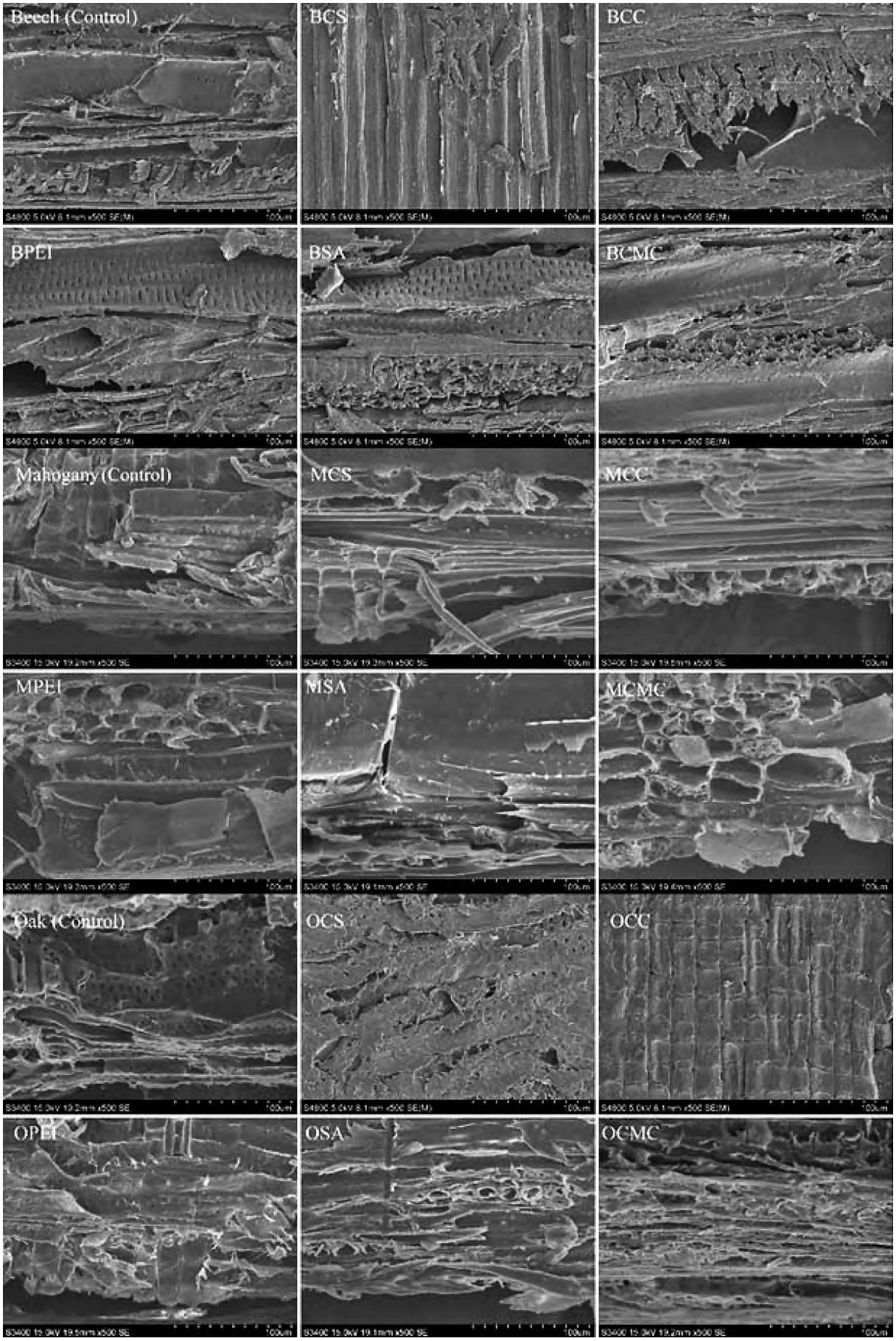

Figure 4 SEM images of functional wood materials
Slika 4. SEM slike funkcionalnih drvnih materijala

ter the impregnation process. On the other hand, it was determined that the surface energies and solubility parameters of the samples decreased depending on the contact angle values. In addition, SEM images proved that the chemicals successfully filled the pores of the wood material. Finally, biomaterials exhibit efficient tribopolarity behavior and may contribute to the applications of the next generation of sustainable smart materials, shedding light on future research studies.

Acknowledgements – Zahvala

The authors thank Dr Jacopo ANDREO and Prof Dr Qi ZHANG as well as BCMaterials (SPAIN) for sample preparation and characterization tests under action CA17128 LignoCost.

The authors would like to thank the Turkish Academy of Sciences & TÜBA for its financial support in this project. The authors would also like to thank the Biomaterials and Nanotechnology Research Group & BioNanoTeam for their valuable contributions during the work.

5 REFERENCES
5. LITERATURA

1. Chen, C.; Song, J.; Zhu, S.; Li, T.; Xie, J.; Hu, L., 2018: Scalable and sustainable approach toward highly compressible, anisotropic, lamellar carbon sponge. Chem, 4: 544-554. https://doi.org/10.1016/j.chempr.2017.12.028
2. Chieng, B. W.; Ibrahim, N. A.; Ahmad Dau, N.; Talib, Z. A., 2019: Chapter 8 – Functionalization of Graphene Oxide via Gamma-Ray Irradiation for Hydrophobic Materials. In: Synthesis, Technology and Applications of Carbon Nanomaterials, Elsevier, pp. 177-203. ISBN 9780128157572
3. Engelund, E. T.; Thygesen, L. G.; Svensson, S.; Hill, C. A., 2013: A critical discussion of the physics of wood – water interactions. Wood Science and Technology, 47: 141-161. https://doi.org/10.1007/s00226-012-0514-7
4. Geffert, A.; Výbohová, E.; Geffertová, J., 2017: Characterization of the changes of colour and some wood components on the surface of steamed beech. Wood Acta Facultatıs Xylologıae Zvolen, 59: 49-57. https://doi.org/10.17423/afx.2017.59.1.05
5. Haleem, N.; Arshad, M.; Shahid, M.; Tahir, M. A., 2014: Synthesis of carboxymethyl cellulose from waste of cotton ginning industry. Carbohydrate Polymers, 113: 249-255. https://doi.org/10.1016/j.carbpol.2014.07.023
6. Huhtamäki, T.; Tian, X.; Korhonen, J. T.; Ras, R. H. A., 2018: Surface-wetting characterization using contact-angle measurements. Nature Protocols, 13: 1521-1538. https://doi.org/10.1038/s41596-018-0003-z
7. Jian, L., 2003. Wood spectroscopy. Beijing: Science and Technology Press.
8. Keplinger, T.; Cabane, E.; Chanana, M.; Hass, P.; Merk, V.; Gierlinger, N.; Burgert, I., 2015: A versatile strategy for grafting polymers to wood cell walls. Acta Biomaterialia, 11: 256-263. https://doi.org/10.1016/j.actbio.2014.09.016
9. Kubovský, I.; Kačíková, D.; Kačík, F., 2020: Structural Changes of Oak Wood Main Components Caused by Thermal Modification. Polymers, 12: 485. https://doi.org/10.3390/polym12020485
10. Lindén, J. B.; Larsson, M.; Kaur, S.; Skinner, W. M.; Miklavcic, S. J.; Nann, T.; Kempsona, I. M.; Nydén, M., 2015: Polyethyleneimine for copper absorption II: kinetics, selectivity and efficiency from seawater. RSC Advances, 5, 51883-51890. https://doi.org/10.1039/C5RA08029K
11. Pal, S.; Mal, D.; Singh, R. P., 2005: Cationic starch: an effective flocculating agent, Carbohydrate Polymers, 59: 417-423. https://doi.org/10.1016/j.carbpol.2004.06.047
12. Rautkari, L.; Hill, C. A.; Curling, S.; Jalaludin, Z.; Ormondroyd, G., 2013: What is the role of the accessibility of wood hydroxyl groups in controlling moisture content. Journal of Materials Science, 48: 6352-6356. https://doi.org/10.1007/s10853-013-7434-2
13. Rodríguez-Fabià, S.; Torstensen, J.; Johansson, L.; Syverud, K., 2022: Hydrophobization of lignocellulosic materials, part II: chemical modification. Cellulose, 29: 8957-8995. https://doi.org/10.1007/s10570-022-04824-y
14. Sun, J.; Tu, K.; Büchele, S.; Koch, S. M.; Ding, Y.; Ramakrishna, S. N.; Stucki, S.; Guo, H.; Wu, C.; Keplinger, T.; Pérez-Ramírez, J.; Burgert, I.; Panzarasa, G., 2021: Functionalized wood with tunable tribopolarity for efficient triboelectric nanogenerators, Matter, 4: 3049-3066. https://doi.org/10.1016/j.matt.2021.07.022
15. Şen, F.; Uzunsoy, İ.; Baştürk, E.; Kahraman, M. V., 2017: Antimicrobial agent-free hybrid cationic starch/sodium alginate polyelectrolyte films for food packaging materials. Carbohydrate Polymers, 170: 264-270. https://doi.org/10.1016/j.carbpol.2017.04.079
16. Şen, F.; Kahraman, M. V., 2018: Preparation and characterization of hybrid cationic hydroxyethyl cellulose/sodium alginate polyelectrolyte antimicrobial films. Polymers for Advanced Technologies, 29: 1895-1901. https://doi.org/10.1002/pat.4298
17. Fernandez, V.; Khayet, M., 2015: Evaluation of the surface free energy of plant surfaces: toward standardizing the procedure. Frontiers in Plant Science, 6: 1-11. https://doi.org/10.3389/fpls.2015.00510
18. Wang, J.; Chen, Y.; Xu, Y.; Mu, J.; Li, J.; Nie, S.; Chen, S.; Xu, F., 2022: Sustainable lignin-based electrospun nanofibers for enhanced triboelectric nanogenerators. Sustainable Energy Fuels, 6: 1974-1982. https://doi.org/10.1039/D1SE02005F
19. Wang, X.; Zhang, Y.; Yu, Z.; Qi, C., 2017: Properties of fast-growing poplar wood simultaneously treated with dye and flame retardant. European Journal of Wood and Wood Products, 75: 325-333. https://doi.org/10.1007/s00107-016-1142-y
20. Zhang, R.; Guo, J.; Liu, Y.; Chen, S.; Zhang, S.; Yu, Y., 2018: Effects of sodium salt types on the intermolecular interaction of sodium alginate/antarctic krill protein composite fibers, Carbohydrate Polymers, 189: 72-78. https://doi.org/10.1016/j.carbpol.2018.02.013
21. Zhu, M. W.; Song, J. W.; Li, T.; Gong, A.; Wang, Y. B.; Dai, J. Q.; Yao, Y. G.; Luo, W.; Henderson, D.; Hu, L. B., 2016: Highly anisotropic, highly transparent wood composites. Advanced Materials, 28: 7563. https://doi.org/10.1002/adma.201600427

Corresponding address:

Assoc. Prof. Dr. MUSTAFA ZOR, PhD
Zonguldak Bulent Ecevit University, Caycuma Vocational School, Department of Forestry, 67900, Zonguldak, TÜRKIYE, e-mail: mustafa.zor@beun.edu.tr